Amphiphilic Poly(organosiloxane) Nanospheres as Nanoreactors for the Synthesis of Topologically Trapped Gold, Silver, and Palladium Colloids

Nadja Jungmann, Manfred Schmidt, and Michael Maskos*

Institut für Physikalische Chemie, Universität Mainz, Welder Weg 11, D-55099 Mainz, Germany

Received September 13, 2002; Revised Manuscript Received April 1, 2003

ABSTRACT: Amphiphilic poly(organosiloxane) nanospheres with different core−shell architectures are employed as passive nanoreactors for the synthesis of noble metal colloids. The amphiphilic poly(organosiloxane) nanospheres, which have diameters between 15 and 40 nm, possess a hydrophilic interior and a hydrophobic shell. Dispersed in organic solvents such as toluene, it has been achieved to transfer hydrophilic noble metal salts through the solvent into the nanospheres by either liquid−liquid or solid−liquid phase transfer. Subsequently, reduction of the noble metal salt with lithium triethylborohydride led to the formation of 2−5 nm sized noble metal colloids. If the network density of the shell of the poly(organosiloxane) nanospheres is small enough, the colloids are topologically trapped inside the nanospheres and stabilized against aggregation. By employing hydrogen tetrachloroaurate(III), silver nitrate, or palladium(II) chloride, it was possible to synthesize topologically trapped gold, silver, or palladium colloids, respectively. The number, the size, and the stability of the colloids depend mainly on (i) the kind of phase transfer chosen, (ii) the amount of hydrophilic groups in the poly(organosiloxane) nanospheres, and (iii) the architecture of the poly(organosiloxane) nanospheres.

Introduction

Monodisperse metals and semiconductor colloids are of growing interest due to their potential application in catalysis, photovoltaic cells, and nonlinear optics. This has led to increasing research activities into the synthesis and stabilization of nanosized particles.[1−8] The classical synthetic routes comprise well-selected ligands[1] or surfactant systems[9,10] to produce monodisperse and stable colloids.

New systems employ block copolymer micelles to stabilize the metal colloids.[11−14] First, the micelles are filled with metal salt, followed by reduction by various reducing agents or by plasma treatment of the absorbed micelles on surfaces.[15] Principally, the block copolymer micelles are subject to fluctuations in size and aggregation number. Another approach is based on preformed gold and silver colloids that were surrounded by a surface network of tetraethoxysilane, although they have not been transferred into organic solvents without particle aggregation.[16−18] Also, dendrimers[19,20] and microgels[21] were employed in the synthesis of metal colloids. Recently, the successful synthesis of active molecular reactors based on poly(organosiloxanes) for the preparation of topologically trapped gold colloids has been reported.[22] The synthesis of other trapped metal colloids has failed, mostly due to slower cluster growth leading to a lack of topological stabilization.

We would like to present passive nanoreactors based on amphiphilic poly(organosiloxane) nanospheres for the synthesis of topologically trapped noble metal colloids. First, we fill the hydrophilic interior of the nanospheres with a metal salt that is subsequently reduced by the addition of a reducing agent. We used poly(organosiloxane) nanospheres with different architectures to analyze the influence of various parameters such as polarity, uptake of metal salt, and stability of the formed metal colloids. The synthesis and characterization of the amphiphilic poly(organosiloxane) nanospheres are described elsewhere.[23] Figure 1 shows a schematic overview of the different spherical architectures of the nanoparticles employed for the synthesis of metal colloids.

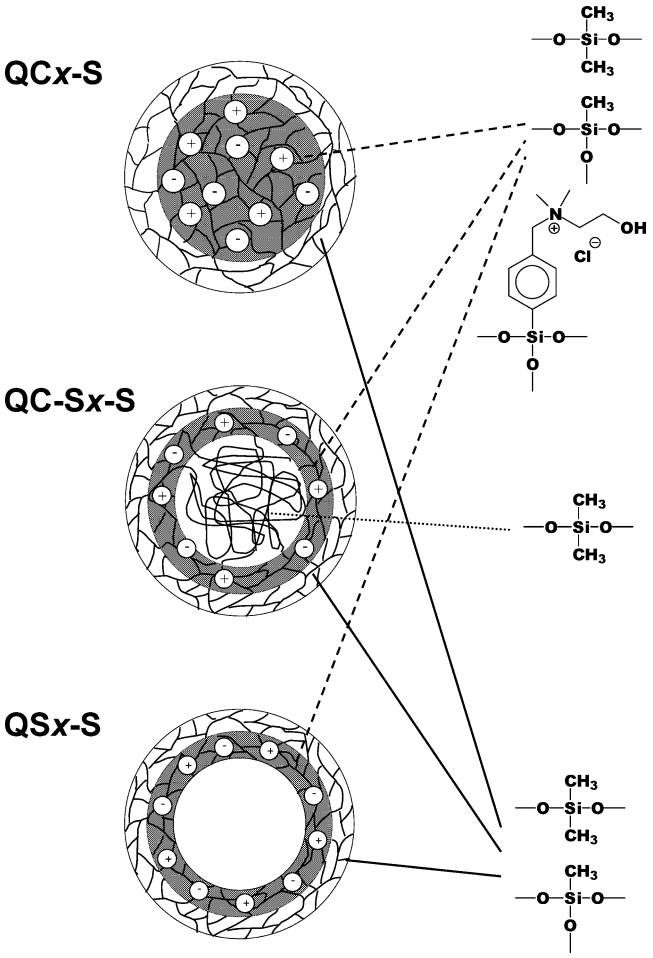

Figure 1. Schematic picture of the amphiphilic poly(organosiloxane) nanospherical networks. The hydrophilic gray part consists of dimethylsiloxane, methylsiloxane, and the quaternary ammonium units; the outer hydrophobic shell is built only by dimethylsiloxane and methylsiloxane units. PDMS chains build the core of QC-S*x*-S. The *x* in the sample code refers to the amount of functional monomer used for the synthesis of the corresponding part of the nanospheres, which later became quaternary ammonium groups.[20]

10.1021/ma021480c CCC: $25.00
Published on Web 04/30/2003

QC*x*-S consists of a core that contains quaternary ammonium groups and is surrounded by the hydrophobic shell. QC-S*x*-S has a core of poly(dimethylsiloxane) (PDMS) chains that are covalently linked to the surrounding inner shell with the quaternary ammonium groups, again surrounded by the hydrophobic shell. When the PDMS chains are not attached to the shell, they can be removed and hollow nanospheres are formed (QS*x*-S).

The amount of quaternary ammonium groups in the hydrophilic part of the amphiphilic poly(organosiloxane) nanospheres, which is indicated by an *x* in the sample code, can be adjusted chemically. The outer shell is in all cases hydrophobic and ensures the solubility of the nanospheres in organic solvents such as toluene. If only alkyltrialkoxysilanes are used in the synthesis, the network is too dense for the penetration of the metal salt through the shell.[22] Therefore, we employed mixtures of dialkyldialkoxysilanes and alkyltrialkoxysilanes.

Experimental Section

The synthesis and characterization of the amphiphilic poly(organosiloxane) nanospheres are described in detail in ref 23. The synthesis is based on the hydrolysis and co-condensation of dialkyldialkoxysilanes (D) and alkyltrialkoxysilanes (T) in aqueous dispersion by sequential addition of monomer mixtures in the presence of a surfactant. Saturation of reactive silanol or silanolate groups prevents the irreversible aggregation of the particles and allows the transfer into toluene as redispersible nanoparticles. The employment of chloromethylphenyltrimethoxysilane (ClBz-T) in the core (C) or in the inner shell (S) results after subsequent polymer-analogous quaternization (Q) with dimethylaminoethanol in the formation of amphiphilic poly(organosiloxane) nanoparticles. The mass fraction of ClBz-T relative to the total amount of monomer is designated by an *x* in the sample code. Thus, QC8-S, for example, is a nanoparticle with a fraction of 8% ClBz-T in the core; with QC-S12-S the nanoparticles have a fraction of 12% ClBz-T in the inner shell. With QC-S*x*-S and QS*x*-S the D units are first condensed to chains, which in the case of QS*x*-S are prevented from reacting with subsequently added monomer by the addition of monoalkoxysilanes. By the use of mixtures of D and T in the construction of the shells, these chains can diffuse out of the interior after transfer into toluene and are removed by ultrafiltration. In QC-S*x*-S the chains remain in the interior since they are bonded covalently to the surrounding shell.

Instrumentation. UV/vis spectra were recorded with a Lambda 17 UV spectrometer (Perkin-Elmer). Transmission electron microscopy was performed with a 420 ST Philips electron microscope at an acceleration voltage of 120 kV.

Materials. Toluene (Merck), hydrogen tetrachloroaurate(III) trihydrate, silver nitrate, palladium(II) chloride (Aldrich), and lithium triethylborohydride (1.0 M solution in THF, Aldrich) were used as received. Water was purified with a Milli-Q deionizing system (Waters).

Synthesis. Solid−liquid phase transfer (see Figure 2a): 5 mL of a solution of poly(organosiloxane) nanospheres ($c = 2.0$ g/L) was added to 10.0 mg of metal salt. Liquid−liquid phase transfer (see Figure 2b): 5 mL of a solution of poly(organosiloxane) nanospheres ($c = 2.0$ g/L) in toluene was added on top of 5 mL of an aqueous solution of metal salt in a glass vial. The concentrations of the metal salts were 53.7 mmol/L for $HAuCl_4$, 159.7 mmol/L for $AgNO_3$, and 152.1 mmol/L for $PdCl_2$. The same experiments were also performed with QC12-S, QC-S12-S, and QS12-S in toluene using an aqueous solution of $HAuCl_4$ with a concentration of only 10.7 mmol/L. All solutions were stored for 2 weeks in the dark. Subsequently, the toluene phase was carefully isolated, and UV/vis spectra were recorded, followed by the reduction of the dispersion with 0.3−0.4 mL of lithium triethylborohydride. Instantaneous coloring was observed for the gold- and silver-containing samples. The samples were analyzed by UV/vis spectroscopy and TEM. Control experiments were also carried out in the same fashion with noncharged spheres (C12-S; for synthesis see ref 23) and toluene. Both showed no detectable UV absorbance in the visible range before and after reduction.

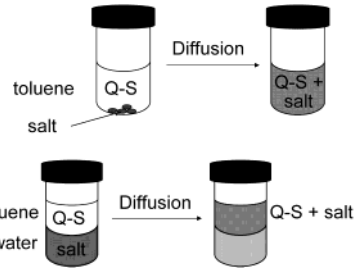

Figure 2. Solid−liquid (top) and liquid−liquid (bottom) phase transfer. Q-S refers to the amphiphilic poly(organosiloxane) nanospheres employed.

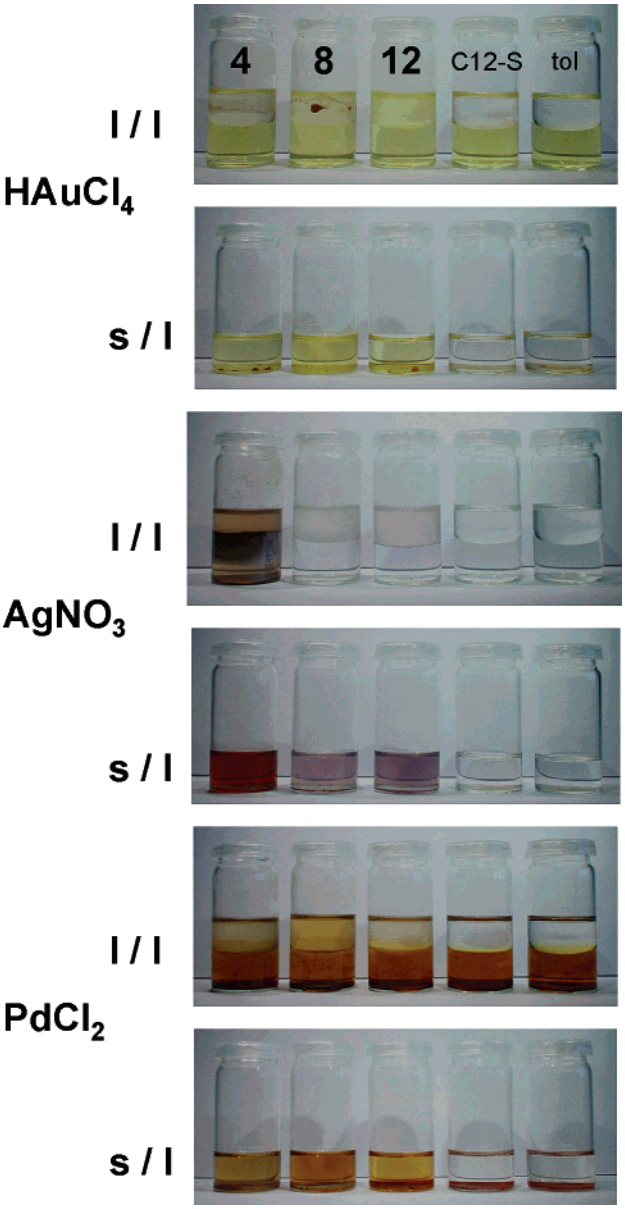

Figure 3. Pictures of the phase transfer of metal salt into the QS*x*-S, dispersed in toluene: l/l = liquid−liquid; s/l = solid−liquid. The numbers in the top row correspond to *x*; for comparison, C12-S and toluene (tol) are also shown (see text).

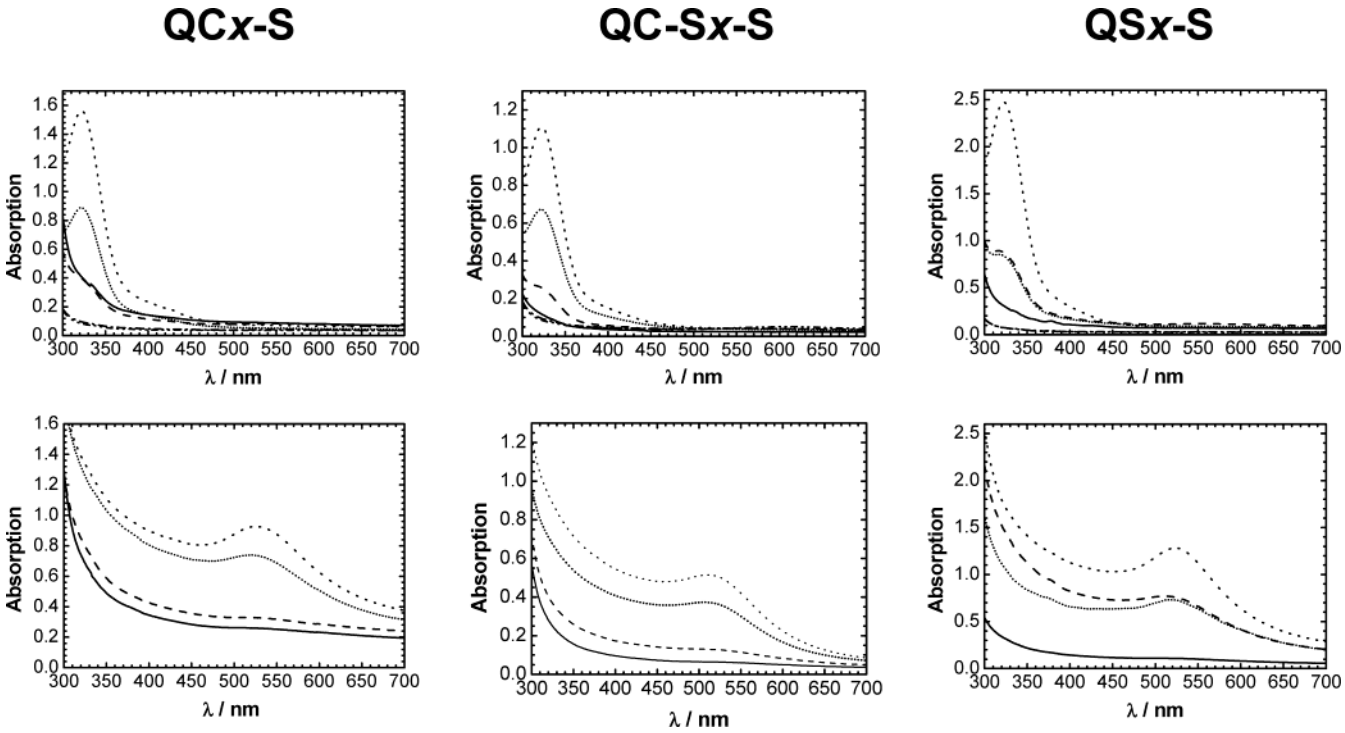

Figure 4. UV/vis absorption spectra of the toluene phase containing the amphiphilic poly(organosiloxane) nanospheres after liquid−liquid phase transfer employing $HAuCl_4$ (starting concentration: $c = 53.7$ mmol/L). Top: before reduction, bottom: after reduction. Solid line: $x = 4$; dashed: $x = 8$; short dashed: $x = 12$; dash−dotted: C12-S; dash−dot-dotted: pure toluene; dotted: $x = 12$, starting concentration of $HAuCl_4$ $c = 10.7$ mmol/L. All solutions have been diluted 1:4 before measurement.

Results and Discussion

The metal salt is transferred into the amphiphilic poly(organosiloxane) nanospheres by solid−liquid (s/l) or liquid−liquid (l/l) phase transfer. Figure 2 shows a schematic picture of the two variants employed. The metal salt is water-soluble and not soluble in toluene, whereas the nanospheres are dispersed in toluene and water-insoluble.

Figure 3 contains pictures of the experiments employing QS-*x*-S nanospheres after 2 weeks. The toluene dispersions containing the amphiphilic nanospheres are colored, whereas the control experiments remain colorless. The hydrogen tetrachloroaurate(III) and palladium(II) chloride solutions turned yellow. The solutions containing silver nitrate also show some coloring, which is mainly due to some slight reduction. UV/vis absorbance spectra of the toluene phase were recorded to quantify the uptake of metal salt into the amphiphilic nanospheres and to analyze the influence of the amount of quaternary ammonium groups inside the nanospheres on the encapsulation. Figure 4 shows the UV/vis spectra for the experiments employing hydrogen tetrachloroaurate(III), which was transferred by liquid−liquid phase transfer.

The typical absorption maximum at $\lambda = 330$ nm is attributed to $HAuCl_4$. The absorption increases with increasing amount of quaternary ammonium groups, independent of the spherical architecture. When comparing the different spherical architectures, it is interesting to note that for the nanospheres with the same amount of quaternary ammonium groups the absolute uptake of $HAuCl_4$ is smallest for QC-S*x*-S, medium for QC*x*-S, and highest for QS*x*-S. The only exception is QS4S, where the uptake is slightly less as compared to QC4-S. A complete analysis is given in Table 1.

The estimation of the mass of incorporated $HAuCl_4$ is performed in the following way. It is observed that when a lower amount of $HAuCl_4$ is offered to QC12-S, QC-S12-S, and QS12-S, the aqueous solutions become completely colorless for QC12-S and QS12-S, as shown in Figure 5.

Table 1. Amount of Hydrogen Tetrachloroaurate(III) Incorporated in 10 mg of the Poly(organosiloxane) Nanospheres (Dispersed in 5 mL of Toluene) by Liquid−Liquid Phase Transfer (91.3 mg of $HAuCl_4$ in 5 mL of Water) Determined by UV−vis Spectroscopy of the Toluene Phase at λ_{max}[a]

sample	mg of $HAuCl_4$ incorp	μmol of $HAuCl_4$	μmol of quat ammon[b]
QC4-S	8.2	24.1	0.7
QC8-S	8.2	24.1	1.1
QC12-S	30.6	90.0	4.6
QC-S4-S	2.9	8.5	1.1
QC-S8-S	6.3	18.5	2.0
QC-S12-S	22.3	65.6	6.2
QS4-S	6.3	18.5	2.2
QS8-S	18.2	53.5	5.0
QS12-S	48.5	142.6	6.5

[a] In relation to the fully incorporated amount of $HAuCl_4$ into QS12-S (18.2 mg). [b] Determined from the amount of quaternary ammonium groups in the nanospheres.[23]

UV/vis spectra of the aqueous phase show nearly no absorption at $\lambda = 330$ nm. Therefore, it is assumed that all the $HAuCl_4$ is transferred into the poly(organosiloxane) nanospheres. The UV/vis spectra of the toluene dispersions are also shown in Figure 4. The UV/vis absorbance at λ_{max} is "calibrated" with the values of QC12-S and QS12-S, where the uptake of $HAuCl_4$ is known. By doing so, the mass uptake of $HAuCl_4$ into the nanospheres is determined for all samples. The highest uptake is obtained for QS12-S, where 10 mg of nanospheres incorporate 48.5 mg of $HAuCl_4$. It is seen that the nanospheres containing the highest amount of quaternary ammonium groups (Table 1) also incorporate the highest amount of $HAuCl_4$ for each individual

Figure 5. Uptake of $HAuCl_4$ into QS-12-S, dispersed in toluene, by liquid−liquid phase transfer (top); starting concentration of $HAuCl_4$ in the water phase: $c = 10.7$ mmol/L (left), $c = 53.7$ mmol/L (right). Bottom: pictures of toluene dispersions of QS-8-S after filling with metal salt by liquid−liquid phase transfer and subsequent reduction. From left to right: gold, silver, palladium.

spherical architecture. Interestingly, an approximately 20-fold excess of incorporated $HAuCl_4$ is determined as compared to the amount of quaternary ammonium groups for QC*x*-S, whereas it is only half for QC-S*x*-S. For QS4-S and QS8-S, also an approximately 10-fold excess is observed, whereas for QS12-S the relative uptake is comparable to QC*x*-S. It is deduced that the microscopic environment is obviously different in the different spherical architectures. The QC-S*x*-S samples and two of the QS*x*-S samples seem to be least attractive for $HAuCl_4$, whereas the QC*x*-S and QS12-S provide an attractive microenvironment for the encapsulation of $HAuCl_4$.

Subsequent reduction leads to the formation of metal colloids. Figure 5 shows pictures of reduced toluene phases obtained after liquid−liquid phase transfer of the corresponding metal salts into QS8-S. The UV/vis spectra for the reduced toluene phases after liquid−liquid phase transfer are also given in Figure 4. The λ_{max} is observed around 520 nm and corresponds to the red color of the solutions. The small differences in λ_{max} and the width of the absorption band resemble among others the difference in size and polydispersity of the gold colloids. Also, the local polarity at the colloidal surface might influence the absorption. This makes it difficult to quantitatively discuss the spectra. Nevertheless, the same trend already observed for the metal salt is also found after reduction.

Table 2. Average Size of the Metal Colloids Determined by TEM

metal	Q-spheres	phase transfer[a]	size [nm]
Au	QC-S8-S	s/l	6.8 ± 6.7
	QC-S12-S	l/l	3.9 ± 2.5
	QS4-S	l/l	3.1 ± 2.6
	QS8-S	l/l	3.2 ± 2.5
Ag	QC4-S	s/l	9.5 ± 14.1
	QC12-S	s/l	5.2 ± 9.4
	QC12-S	l/l	3.1 ± 4.7
	QC-S12-S	l/l	4.3 ± 3.7
	QC-S12-S[b]	l/l	4.1 ± 5.1
	QS8-S	l/l	3.5 ± 4.0
Pd	QC12-S	s/l	5.0 ± 4.0
	QC12-S	l/l	3.9 ± 4.6
	QC-S8-S	l/l	3.9 ± 2.1
	QS8-S	s/l	4.3 ± 4.8
	QS8-S	l/l	4.1 ± 2.4

[a] s/l: solid−liquid; l/l: liquid−liquid. [b] Lower amount of silver nitrate offered ($c = 31.9$ mmol/L); see experimental part.

The solid−liquid phase transfer also yields colored solutions, as can be seen in Figure 3. The uptake of $HAuCl_4$ shows principally the same dependencies on the architecture or the amount of quaternary ammonium groups as it was observed for the liquid−liquid phase transfer. The amount of $HAuCl_4$ encapsulated as determined by UV/vis spectroscopy is smaller as compared to the corresponding liquid−liquid phase transfer.

The encapsulation of Pd(II) chloride yields comparable results before the reduction. After reduction, the absorption of the colloids is shifted into the UV region below 300 nm and cannot be detected. The scattering at higher λ again follows the trend already observed before the reduction. The immediate reduction of silver nitrate makes it impossible to determine the uptake into the nanospheres quantitatively with UV/vis spectroscopy.

After reduction, the nanospheres and the formed metal colloids are analyzed with transmission electron microscopy. Figure 6a shows gold colloids formed after solid−liquid (top) and liquid−liquid (bottom) phase transfer, followed by the reduction with lithium triethylborohydride.

Interestingly, most of the gold colloids are not in the nanospheres but attached to their outside in the case of the solid−liquid phase transfer. Nevertheless, the dispersions are stable and no macroscopic gold is formed. In contrast to this, the gold colloids are found mostly inside the nanospheres for the liquid−liquid phase transfer, although the size distribution of the metal colloids is not monodisperse. The size analysis for the metal colloids generated in the amphiphilic poly(organosiloxane) nanospheres is summarized in Table 2.

For the solid−liquid phase transfer it is observed for all metals that the size of the metal colloids is comparably large and very broad. This can also been seen in Figure 6b,c for silver and palladium, where some of the colloids are located inside the nanospheres, but also many larger ones are found outside. Again, the dispersions are nevertheless stable.

The liquid−liquid phase transfer yields nearly all metal colloids entrapped in the nanospheres for both silver and palladium. Especially in the case of silver, nearly all nanospheres contain one silver colloid. For gold and palladium, also one colloid is observed per nanospheres, but it seems that not all nanospheres are

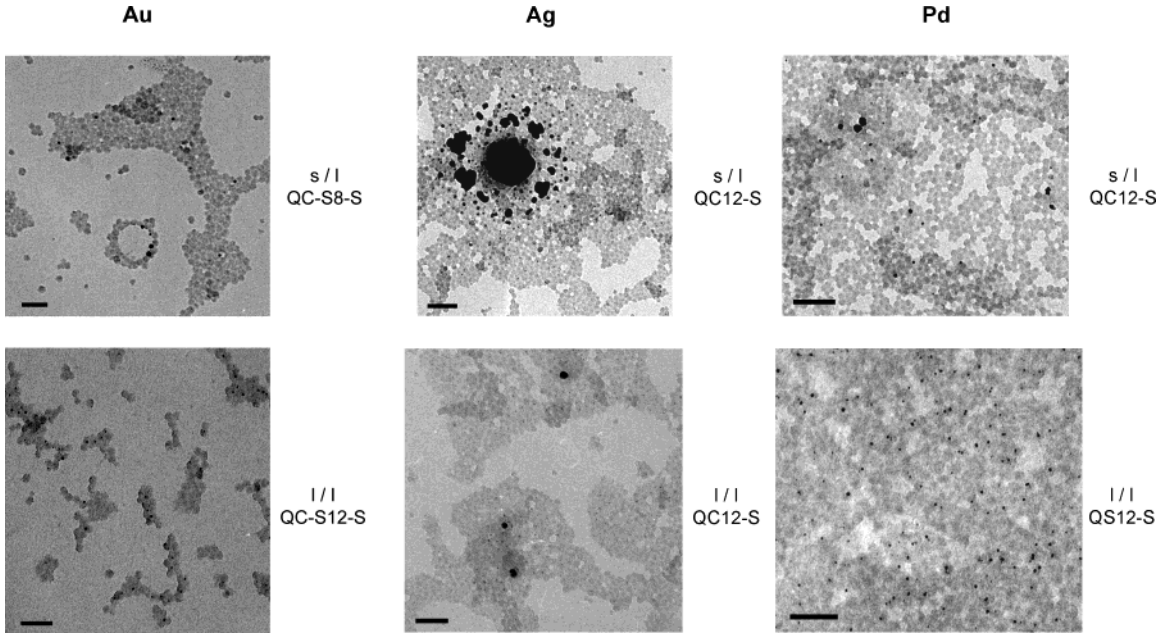

Figure 6. TEM pictures obtained from the toluene phase after solid−liquid (top) or liquid−liquid (bottom) phase transfer into the amphiphilic nanospheres and subsequent reduction (scale bar: 100 nm): (a) gold; (b) silver; (c) palladium.

filled. The average size of the colloids is found to be between 3.1 and 4.3 nm, independent of the metal employed. These observations lead to the following conclusions. First, the stabilization of the metal colloids inside the nanospheres depends on the kind of phase transfer. The presence of water definitely promotes the encapsulation of the metal salt. Second, the size of the metal colloids is in the case of the liquid−liquid phase transfer mainly determined by the network density of the shell, which is comparable for all the different architectures, although the absolute loading is found to depend on the architecture of the nanospheres, as was shown for $HAuCl_4$. To test this hypothesis, nanospheres with different network density were synthesized. These Q(S12-S)* spheres contain the same amount of quaternary ammonium groups in the inner shell as compared to QS12-S, but the rest of the inner shell is not an equal mixture of dimethylsiloxy and methylsiloxy groups, but contains a 3.5-fold excess of the dimethylsiloxy groups, meaning that the inner shell is less dense as compared to QS12-S. The outer shell on the other hand contains 70% of methylsiloxy groups in the case of QS12-S and 75% for Q(S12-S)*, which leads to higher density for the latter. The liquid−liquid phase transfer of $HAuCl_4$ into Q(S12-S)* is also analyzed by TEM. Figure 7 shows that each nanosphere contains at least one small gold colloid; some contain even several. The average size of the gold colloids is determined to 1.7 ± 0.7 nm. The size and also the polydispersity are definitely smaller than for the other nanospheres.

This observation underlines the influence of the outer shell and also promotes the theory of nucleation and particle growth already introduced for the active nanoreactors.[22] The metal salt is first reduced to atomic metal that in a following step aggregates to form growing nuclei. Stable metal colloids are obtained if this process is fast enough to grow colloids that are topologically trapped in the amphiphilic nanospheres. Otherwise, the precursor or the growing colloids diffuse out of the poly(organosiloxane) network and form larger colloids. The presence of water also seems to influence the colloidal synthesis. First, the uptake of metal salt after solid−liquid phase transfer is lower as compared to the water-containing system, and second, the growing colloids are less topologically trapped. This may be attributed either to the already lower metal salt content in the nanospheres, leading to fewer colloids and increased possibility to diffuse out of the nanospheres, or to the presence of water, which might act as additional stabilizer in the process of colloid formation. The presence and influence of water will be the subject of future studies.

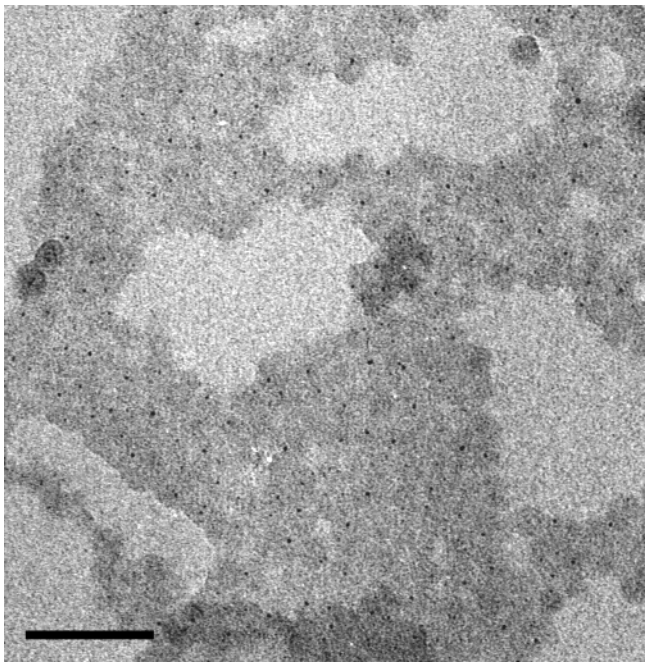

Figure 7. TEM picture obtained from the toluene phase after liquid−liquid phase transfer of $HAuCl_4$ into Q(S12-S)* and subsequent reduction (scale bar: 100 nm).

Conclusions

Amphiphilic poly(organosiloxane) nanospheres were successfully employed in the synthesis and stabilization

of gold, silver, and palladium colloids. The metal colloids are topologically trapped inside the nanospheres after liquid−liquid phase transfer of the corresponding metal salt and subsequent reduction, whereas after solid−liquid phase transfer, most of the colloids are found outside the nanospheres. The uptake of metal salt increases with increasing amount of quaternary ammonium groups in the nanospheres. Therefore, the incorporation of metal salt may be controlled and adjusted. Also, it has been shown that the architectures of the spherical nanoparticles determine the encapsulation of metal salt. Here, QC-S*x*-S shows the lowest content, followed by QC*x*-S. The highest uptake is observed for QS*x*-S, leading in the case of $HAuCl_4$ to an incorporation of 48.5 mg in 10.0 mg of QS12-S nanospheres. After reduction, this corresponds to 28.1 mg of encapsulated colloidal gold. Finally, it was shown that the cross-link density of the outer shell also influences the topological entrapment of the growing colloids. An outer shell with increased network density leads to smaller and less polydisperse colloids.

Acknowledgment. We thank Rudolf Würfel for his help with the TEM measurements and the BMBF (FKZ 03C0288A8) and the Wacker Chemie for financial support.

References and Notes

(1) Schmid, G. *Chem. Rev.* **1992**, *92*, 1709.
(2) Weller, H. *Adv. Mater.* **1993**, *5*, 88.
(3) Henglein, A. *Chem. Res.* **1989**, *89*, 1861.
(4) Wang, Y. *Acc. Chem. Res.* **1991**, *24*, 133.
(5) Toshima, N.; Wang, Y. *Adv. Mater.* **1994**, *6*, 245.
(6) Toshima, N.; Yonezawa, T. *Makromol. Chem., Macromol. Symp.* **1992**, *59*, 281.
(7) Nakahira, T.; Grätzel, M. *J. Phys. Chem.* **1984**, *88*, 4006.
(8) Lewis, L. N.; Wengrovins, J. H.; Burnell, T. B.; Rich, J. D. *Chem. Mater.* **1997**, *9*, 761.
(9) Fendler, J. H. *Adv. Polym. Sci.* **1994**, *113*, 1.
(10) Reetz, M. T.; Helbig, W. *J. Am. Chem. Soc.* **1994**, *116*, 7401.
(11) Förster, S.; Antonietti, M. *Adv. Mater.* **1998**, *10*, 195.
(12) Selvan, S. T.; Spatz, J. P.; Klok, H.-A.; Möller, M. *Adv. Mater.* **1998**, *10*, 132.
(13) (a) Moffit, M.; McMahon, L.; Pessel, V.; Eisenberg, A. *Chem. Mater.* **1995**, *7*, 1185. (b) Moffit, M.; Vali, H.; Eisenberg, A. *Chem. Mater.* **1998**, *10*, 1021.
(14) Mayer, A. B. R. *Polym. Adv. Technol.* **2001**, *12*, 96.
(15) Spatz, J. P.; Mossmer, S.; Möller, M.; Herzog, T.; Plettl, A.; Ziemann, P. *J. Lumin.* **1998**, *76*, 168.
(16) Liz-Marzán, L. M.; Giersig, M.; Mulvaney, P. *Chem. Commun.* **1996**, *6*, 731.
(17) Ung, T.; Liz-Marzán, L. M.; Mulvaney, P. *Langmuir* **1998**, *14*, 3740.
(18) Giersig, M.; Ung, T.; Liz-Marzán, L. M.; Mulvaney, P. *Adv. Mater.* **1997**, *9*, 570.
(19) Ensumi, K.; Suzuki, A.; Aihara, N.; Usui, K.; Torigoe, K. *Langmuir* **1998**, *14*, 3157.
(20) Gröhn, F.; Bauer, B. J.; Akpalu, Y. A.; Jackson, C. L.; Amis, E. J. *Macromolecules* **2000**, *33*, 6042.
(21) Antonietti, M.; Gröhn, F.; Hartmann, J.; Bronstein, L. *Angew. Chem., Int. Ed. Engl.* **1997**, *36*, 2080.
(22) Roos, C.; Schmidt, M.; Ebenhoch, J.; Baumann, F.; Deubzer, B.; Weis, J. *Adv. Mater.* **1999**, *11*, 761.
(23) Jungmann, N.; Schmidt, M.; Maskos, M.; Ebenhoch, J.; Weis, J. *Macromolecules* **2002**, *35*, 6851.

MA021480C